Ecological Indicators 154 (2023) 110719

Contents lists available at ScienceDirect

Ecological Indicators

journal homepage: www.elsevier.com/locate/ecolind

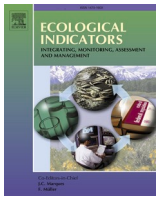

Combination of multiple stable isotope and elemental analyses in urban trees reveals air pollution and climate change effects in Central Mongolia

Enkh-Uchral Batkhuyag [a,b], Marco M. Lehmann [b], Paolo Cherubini [b,c], Bilguun Ulziibat [a,d], Tseren-Ochir Soyol-Erdene [a], Marcus Schaub [b], Matthias Saurer [b,*]

[a] Research Laboratory of Environmental Chemistry and Geochemistry, National University of Mongolia, Ulaanbaatar, Mongolia
[b] Swiss Federal Institute for Forest, Snow and Landscape Research WSL, Birmensdorf, Switzerland
[c] Department of Forest and Nature Conservation, Faculty of Forestry, University of British Columbia, Vancouver BC, Canada
[d] Institute of Geography and Geoecology, Mongolian Academy of Sciences, Ulaanbaatar, Mongolia

ARTICLE INFO

Keywords:
Ulaanbaatar
Air pollution
Stable isotope analyses
Tree rings
Trace elements
Leaves
Climate change
Tree physiology

ABSTRACT

The Ulaanbaatar area in Mongolia has become one of the most polluted regions worldwide due to the rapid increase in urbanization, industrial activity and traffic. However, we critically lack knowledge on the impacts of air pollution on surrounding forest ecosystems that may be further amplified by the ongoing climate change. Here, we apply a novel combination of multiple stable isotope analyses (nitrogen: $\delta^{15}N$, carbon: $\delta^{13}C$, oxygen: $\delta^{18}O$, hydrogen: $\delta^{2}H$) in foliar and tree-ring samples from different tree species, including deciduous, broadleaf species (poplar and birch), a deciduous conifer (larch) and needle evergreen species (spruce and Scots pine). This was complemented by trace element analysis, to study the influence of air pollution and climate on urban, suburban and more remote forests in and around Ulaanbaatar. We found indications of pollution effects in urban and suburban sites in foliar material, particularly in $\delta^{15}N$, with unusually high values of $> 10‰$, that could be related to tree uptake of NO_x. Results were similar for all species, but with a smaller effect for Scots pine. The tree-ring $\delta^{15}N$ values were found to be clearly enriched in recent years compared to 50 years ago at the urban sites, consistent with a pollution signal. Leaves and needles at suburban and urban sites had accumulated higher concentrations of various trace elements including Al, B, Ba, Ca, Cr, Cu, Fe, Mg, Na, S and Zn compared to the more distant sites, confirmed by Principal Component Analysis. Our data on $\delta^{13}C$, $\delta^{18}O$ and $\delta^{2}H$ enabled us to infer possible physiological effects induced by air pollution. Consistently increasing tree-ring $\delta^{13}C$ values over recent decades for all investigated species indicated increasing plant stress, like hampered stomatal conductance and photosynthesis, but this was found for all sites, suggesting climate change rather than air pollution effects. In summary, we show that our multi-isotope and -element approach provides new insights into the threats to forests in urban areas, where the occurrence of more frequent droughts acts together with air pollution.

1. Introduction

Air pollution is of major concern for the society in Mongolia, which is one of the most rapidly developing countries in Asia (Allen et al., 2013; WHO, 2019). Increased industrial activities and expanding human population have resulted in growing emissions of pollutants, enhanced by secondary aerosol formation (Barabad et al. 2018; Nishikawa et al. 2011), affecting not only ecosystems, but also human health (Lelieveld et al. 2015). During the last two decades, air pollution has increased to such an extent that Ulaanbaatar during wintertime was reported as one of the most polluted cities in the world (UNICEF 2018). Recently, forest decline has been observed at Mt. Bogdkhan near Ulaanbaatar, suspected to be related to air pollution (Sase et al. 2005). Sulfur content of the needles from larch trees (*Larix sibirica*) were two times higher on the slope facing a power plant than in more distant areas, which suggests that the observed forest decline is driven by increased SO_2 emission levels from industrial activity (Dulamsuren et al. 2009; Sase et al. 2005).

Furthermore, forests in Mongolia suffer not only from air pollution, but also from extreme climate events, such as frost or extended drought and heat events (Leland et al. 2023). On the Mongolian Plateau, a recent decade-long drought that exceeded the variability of the instrumental record, associated with economic, social, and environmental changes,

* Corresponding author.
E-mail address: matthias.saurer@wsl.ch (M. Saurer).

https://doi.org/10.1016/j.ecolind.2023.110719
Received 4 April 2023; Received in revised form 20 July 2023; Accepted 21 July 2023
Available online 26 July 2023

was recorded (Hessl et al. 2018). As a result, the forest area in Mongolia has significantly decreased during recent decades under the combined effects of natural and anthropogenic factors (Juřička et al. 2020). Studying the combined effects of air pollution and climate change on urban and *peri*-urban forest ecosystems in Mongolia is crucial to gain more information on their health status, risk of decline (Cailleret et al. 2018; Cherubini et al. 2021), and response to climatic variability, in order to assess appropriate management measures (Hauck et al. 2016; Sase et al. 2005; Takahashi et al. 2020).

The stable isotopic composition of plant organic matter as well as the trace elemental composition have been used to quantify sources and effects of atmospheric pollution on vegetation, either in the short term using needles or in the long term based on tree rings (Griffiths 2020; Savard et al. 2004; Siegwolf et al. 2001). Due to the relatively depleted heavy isotope ^{13}C relative to ^{12}C in fossil fuels, expressed as $\delta^{13}C$, their combustion results in a long-term decline in the atmosphere globally (Belmecheri and Lavergne 2020), but can also lead to more ^{13}C-depleted CO_2 in strongly polluted urban areas compared to rural areas (Newman et al. 2008). Furthermore, carbon isotope fractionations of plants during photosynthesis are modified under stress, e.g., by reduced stomatal conductance and subsequently enhanced water-use efficiency, which results in relatively higher $\delta^{13}C$ values of organic matter, like leaves (Farquhar et al. 1989). Such changes are also recorded in the isotope ratio of tree rings which enables their reconstruction over long time scales (Büntgen et al. 2021; Kress et al. 2010). The consideration of oxygen ($\delta^{18}O$) and hydrogen ($\delta^{2}H$) isotope ratios in plant material provides further insight into hydrological processes in the atmosphere as well as during ecosystem evaporation and transpiration (Cernusak et al. 2016), but also air pollution effects (Siegwolf et al. 2022). Nitrogen isotope ratios ($\delta^{15}N$) have previously been used to distinguish between two main N pollution sources, NOx from combustion processes and NHx from agriculture (Saurer et al. 2004). The nitrogen cycle in ecosystems is complex and many fractionation processes in the soil, e.g. microbial processes, affect the isotope ratio of soil N, which is the main source of N for plants (Högberg et al. 2011; McLauchlan and Craine 2012). Despite this complexity, uptake of atmospheric N-compounds through stomatal pores has been shown to significantly affect leaf and wood $\delta^{15}N$ values under conditions of high pollution (Savard et al. 2023). Generally, higher $\delta^{15}N$ values have been reported for the main urban N-deposition form (NOx) compared to the main rural and agricultural N-deposition form (NHx). The relationship between plant $\delta^{15}N$ and N concentrations in different plant species and at varying spatial scales were investigated and their combined analysis was proven to be helpful for a better understanding of nitrogen uptake (Cobley and Pataki 2019; Gerschlauer et al. 2019; Saurer et al. 2004). However, the combination of all these stable isotope ratios (C, O, H, N) has so far hardly been applied, but could be useful to better trace anthropogenic contaminations sources (traffic emissions or industrial production) and detect physiological responses of the trees to air pollution and climate.

Furthermore, the use of trace elemental analysis is useful to monitor air pollution effects on trees (Maher et al. 2008; McLaughlin et al. 2002). Emissions from different sources like road traffic activities, soil dust or industrial activity may be differed by their typical trace elemental compositions, e.g., Cu, Zr, Sb, Ba for brake wear, Fe for other traffic-related emissions, Si, Ca for resuspended dust, and Cr, Ni for industrial emissions (Visser et al. 2015). Accordingly, various species and plant parts have already been used as biomonitors, as particulate matter is not only deposited on leaf surfaces, but is able to enter plants either by the roots (Cutter and Guyette 1993), or through leaves (Ballikaya et al. 2023; Cocozza et al. 2019). For instance, micro and macro-elements in leaves of three broadleaf tree species were analysed (Kardel et al. 2018) and Al, Fe, Ti, Co, Cr, Cu, Ni, Rb, Si, V, Zn and Zr attributed to emissions from road traffic activities and Mn and Sb to industrial activity. Dendrochemistry is the analysis of trace elements in wood and, in combination with tree-ring analysis, can provide past levels of contamination (Dinis et al. 2021; Guyette et al. 1991; McLaughlin et al. 2002). This method enables to trace pollutants on a spatial and temporal scale in relation to their sources (Austruy et al. 2019; Ballikaya et al. 2022), but leaves may still be the most direct and reliable recorder of pollution levels (Salehi et al. 2020).

The aims of this study were applying a novel combination of multiple stable isotope and element analyses of needles and leaves from different tree species growing in or around the city of Ulaanbaatar to detect possible pollution effects, and to link them to long-term changes by applying the same method to tree rings. Specifically, we assessed 1) how sensitively different tree species are recording air pollution, 2) how this impact has changed over the recent decades, and 3) how much trees are affected physiologically today by the combined influence of climate and air pollution.

2. Materials and methods

2.1. Air pollution and climate in the study area

The study area is located in and around Ulaanbaatar (49°74′N, 106°79′E) as shown in Fig. 1. Ulaanbaatar, the capital city of Mongolia with 1.5 million inhabitants, is located in north-central Mongolia in a basin at around 1300 m a.s.l., surrounded by mountains in the north (Chingeltei Khairkhan, 1947 m a.s.l) and the south (Bogd Khan, 2250 m a.s.l). The Tuul river runs through the valley from the east to the west. The rapid growth of Ulaanbaatar city and the significant population migration from rural areas contributed to the massive increase of air pollution levels during the last three decades.

Particularly during the cold season (from November to February), high levels of pollution are observed. This is due to the geographical location of the city in a depression and the temperature inversion under the Siberian high-pressure system obstructing air circulation (Ganbat et al. 2020; Kolář et al. 2020). The most abundant air pollutants in winter are sulfur dioxide (SO_2), nitrogen dioxide (NO_2) and particulate matter (PM), as a result of the high emissions from fossil fuel and biomass combustion for heating and domestic needs (Davy et al. 2011). During the past two decades, pollutants such as SO_2, NO_2 and PM have been higher than the standards set by the World Health Organization (WHO) guidelines (Ganbat et al. 2020). In particular, extremely worrisome is the fact that atmospheric SO_2 does not show a decreasing trend in Ulaanbaatar, in contrast to most cities in East Asia (Takahashi et al. 2020).

As recorded during the period 1960 to 2019 (*CRU TS4.04*), mean annual temperature and precipitation were -2.2 ± 0.9 °C and 304 ± 54 mm (mean ± deviation), respectively. Around 70% of the total precipitation falls in the summer, between June and August. The meteorological records show warming trends in our study area during the past decades.

2.2. Sampling sites

In the vicinity of Ulaanbaatar city, we selected four study sites (Fig. 1B): two in the city (Suburban, Urban) dominated by *Larix sibirica* (larch), *Pinus sylvestris* (Scots pine), and *Populus tremula* (poplar) and two in mixed forests sites located in the mountains, north of Ulaanbaatar at Khalzangiin Davaa (Mt.A) and at Bogd Khan (Mt.B), south of Ulaanbaatar, with altitudes ranging from 1200 to 1600 m a.s.l, dominated by *Betula platyphylla* (birch), *Larix sibirica*, *Pinus sylvestris*, and *Picea obovata* (spruce). Suburban is a complex area that includes industrial, commercial, and residential areas, with varying traffic intensity. Mt.B is the closest forest area to Ulaanbaatar and comprises two separate locations for our study (Fig. 1B). Mt.A as the most distant from the city and opposite to the general wind direction can be assumed to be the least polluted site. The distance of the sub-urban sites to the city center is ca. 5 km, the two sites at Mt.B are each ca. 15 km away from the city, while Mt.A is ca. 25 km distant.

All samples in this study were collected in the summer (end of July to

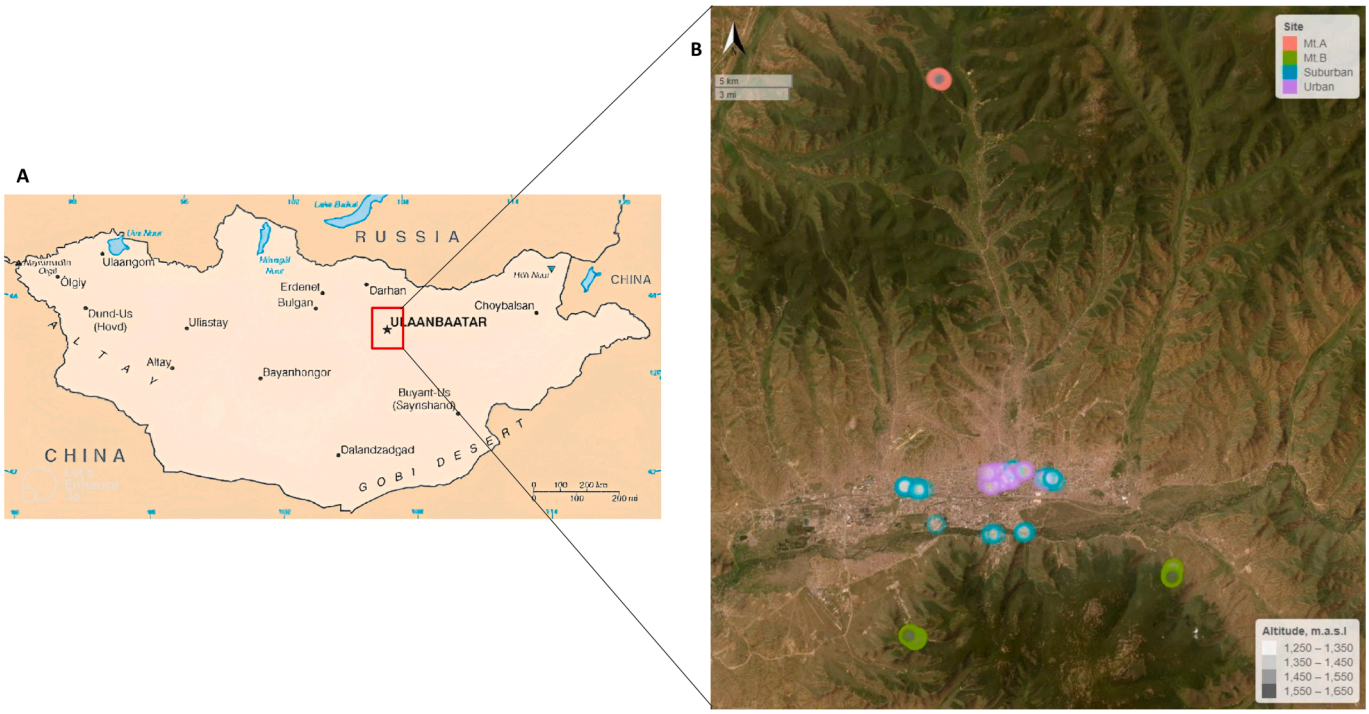

Fig. 1. Study area in Mongolia (A) and sampling sites (B). The circles on the detailed map B are color-coded according to the altitude (inner color) and site location (outer ring).

the beginning of August in 2020) (Table 1). Twigs with leaves and needles were sampled in paper bags following Rautio et al. (2020). Specifically, current year needles were collected. The samples were then stored in a cool box, and air-dried. Two cores from each tree were sampled at breast height (1.3 m), using an increment borer with 5 mm internal diameter. All tree-ring cores were dried, polished and cross-dated following standard dendrochronological methods. The cross-dating measurements were tested and corrected using the COFECHA program (Holmes 1983). The tree-ring width (TRW) was measured using the WinDENDRO program with 0.001 mm resolution. TRW indices were calculated as residuals from estimated growth curves after applying a spline method to the raw measurement series.

2.3. Elemental analysis

Dried leaves and needles and woody samples were homogenized by ball-mill ("Retsch" MM 400, Germany) with a frequency of 30 times per second for one minute using metal-free zirconium oxide ball and tube. For the sample pre-treatment, mixtures of nitric acid (5 M, HNO_3) and hydrofluoric acid (0.5 M, HF) were added to the dried and ground plant materials and placed in a microwave (Ultraclave IV, MLS GmbH) under pressure in order to digest the samples completely (Salehi et al. 2020). In total, nineteen elements including aluminum (Al), boron (B), barium (Ba), calcium (Ca), chromium (Cr), copper (Cu), iron (Fe), potassium (K), magnesium (Mg), manganese (Mn), molybdenum (Mo), sodium (Na), nickel (Ni), phosphorus (P), sulfur (S) and zinc (Zn) were measured in leaves/needles samples by Inductively Coupled Plasma Optical Emission Spectrometry (ICP-OES Optima 7300 DV, Perkin Elmer) in the

Table 1
General characteristics of site, tree species and needle isotope composition in the different sampling areas. Values are given as averages (±standard deviation for isotope and % values).

Sites/Species	n	Altitude, m a.s.l	Height, m	Diameter, cm	$\delta^{15}N$, ‰	$\delta^{13}C$, ‰	$\delta^{18}O$, ‰	$\delta^{2}H$, ‰	C, %	N, %	C/N
Mt.A											
Birch	5	1554	19.6	25.8	−3.9 ± 1.9	−29.8 ± 1.3	19.9 ± 1.7	−190 ± 8	43.0 ± 1.2	2.3 ± 0.2	18.5
Larch	5	1542	23.4	43.7	0.6 ± 2.3	−29.3 ± 0.6	22.0 ± 0.7	−182 ± 3	44.6 ± 0.4	1.8 ± 0.2	24.4
Scots Pine	5	1555	21.5	42.5	−3.8 ± 1.4	−27.0 ± 0.7	23.4 ± 0.9	−167 ± 6	48.5 ± 0.7	1.5 ± 0.2	35.5
Mt.B											
Birch	15	1559	13.8	21.5	0.6 ± 1.2	−29.7 ± 0.9	22.1 ± 1.1	−167 ± 9	43.8 ± 0.7	2.6 ± 0.2	17.0
Larch	15	1527	19.0	42.8	1.9 ± 1.4	−27.7 ± 1.0	23.4 ± 0.7	−170 ± 8	44.9 ± 0.6	2.3 ± 0.2	20.1
Spruce	10	1551	19.4	37.5	2.3 ± 1.6	−26.6 ± 1.3	27.0 ± 0.8	−153 ± 9	45.4 ± 0.8	1.2 ± 0.1	37.0
Scots Pine	15	1564	16.4	41.7	1.2 ± 1.7	−26.2 ± 1.1	24.7 ± 0.9	−152 ± 10	47.8 ± 0.7	1.4 ± 0.1	34.6
Suburban											
Larch	4	1314	13.6	24.6	10.0 ± 2.3	−27.0 ± 0.5	23.3 ± 1.9	−163 ± 11	43.8 ± 0.7	2.8 ± 0.7	16.4
Poplar	16	1292	15.2	31.2	7.9 ± 3.1	−29.7 ± 1.3	21.7 ± 1.4	−137 ± 13	39.8 ± 1.4	2.6 ± 0.4	15.9
Scots Pine	5	1293	5.9	8.2	4.7 ± 1.9	−26.2 ± 0.5	24.1 ± 1.5	−176 ± 10	47.5 ± 0.9	1.3 ± 0.0	36.8
Urban											
Larch	7	1303	15.4	32.5	11.1 ± 1.1	−28.1 ± 0.8	24.5 ± 0.8	−157 ± 7	42.6 ± 0.9	2.1 ± 0.3	20.3
Spruce	5	1304	15.0	25.3	11.3 ± 0.8	−27.5 ± 0.6	29.3 ± 0.7	−147 ± 17	44.6 ± 1.3	1.7 ± 0.6	28.5
Poplar	5	1309	15.1	36.5	13.3 ± 3.1	−30.4 ± 1.8	20.0 ± 1.9	−140 ± 18	39.9 ± 1.8	2.8 ± 0.4	14.3
Scots Pine	5	1301	9.4	18.0	5.1 ± 4.3	−27.0 ± 0.5	25.4 ± 1.7	−159 ± 14	46.8 ± 1.1	1.4 ± 0.1	33.8
Total	**117**										

laboratories of WSL, Switzerland. Each measurement was replicated three times.

2.4. Stable isotope analysis

Homogenized plant materials as whole leaves and needles and wood samples were prepared for isotopic analysis. For wood samples, separate cores of 5 trees per site were extracted with ethanol using Soxhlet apparatus during 24 h to remove resins. The dried cores were then split into ten-year increments for the last six decades (1960–2019) and each increment of each tree was separately ball-milled for isotope analysis. For the determination of the $\delta^{15}N$ and $\delta^{13}C$, 0.9–1.1 mg samples were weighted into tin capsules, combusted in an elemental analyser and measured in a Sercon 2020 Isotope ratio mass-spectrometer (IRMS). The precision of the analysis was 0.3‰ for $\delta^{15}N$ and 0.1‰ for $\delta^{13}C$. For $\delta^{2}H$ and $\delta^{18}O$-analysis, the same amount of samples were weighted using silver capsules, equilibrated with water of known isotopic composition to account for exchangeable hydrogen-groups (Schuler et al. 2022) and measured by thermal decomposition at 1420 °C with a TC/EA (Elementar, Hanau, Germany) connected to an IRMS (Delta XP, Thermo). The precision of the analysis was 2‰ for $\delta^{2}H$ and 0.2‰ for $\delta^{18}O$. Tree-ring $\delta^{13}C$ values were corrected for the so-called Suess effect, the trend in global background atmospheric $\delta^{13}C$ values of CO_2 due to the increasing CO_2 concentration originating mainly from fossil fuel combustion (Belmecheri and Lavergne 2020). This was done after calculation of ten-year averages of the atmospheric correction corresponding to our tree-ring values (1960–69, 1970–79, 1980–89, 1990–99, 2000–2009, 2010–2019).

2.5. Statistical analysis

Significant differences in concentrations of chemical elements in needles of larch and Scots pine from four different sites were tested t-tests, separately. In order to evaluate the relationship between $\delta^{15}N$ composition and N content for each species, the Pearson's correlation analysis was used. The Principal Component Analysis (PCA) was used to investigate the concentration of chemical composition in needles of larch and Scots pine and calculate the significant correlation with the macro- and micro element concentrations in studied sites. All statistical analyses were performed using R and RStudio (Version 4.0.3) with "ggplot", "Factoextra", "Factominer" packages. The statistical significance of the trends was assessed using R (R-Core-Team 2020) and the package "treeclim".

3. Results

3.1. Stable isotope composition of foliar materials

The average $\delta^{13}C$ varied between the studied species, consistently across all sites, and were most negative for the deciduous, broadleaf species poplar and birch (-29.7‰ to −30.4‰), intermediate for the deciduous conifer larch (-27.0‰ to −29.3‰), and highest for the needle evergreen species spruce and Scots pine (-26.2‰ to −27.5‰) (Table 1, Fig. 2A). In contrast to these differences between species, there were no significant differences between the sites for $\delta^{13}C$ when comparing the same species (Table 1).

For $\delta^{15}N$, the composition varied over a large range of −5‰ to + 15‰ across all study sites and species, with a mean of 3.67 ± 4.5‰. No significant differences between species were observed when combining the data from all sites (Fig. 2B). In contrast to the $\delta^{13}C$ results, however, the site differences were clear for $\delta^{15}N$. The average $\delta^{15}N$ values in needles of larch, one of the species measured at all 4 sites, were significantly lower ($p < 0.01$) at Mt.A and Mt.B (0.6‰ to 1.9‰) compared to suburban and urban sites (9.9‰ to 11.1‰). This gradient was also observed for Scots pine, but to a smaller degree (-3.8‰ to 1.2‰ vs. 4.7‰ to 5.1‰). Strongly enriched $\delta^{15}N$ values above 10‰ at urban and suburban sites were also found for spruce and poplar (Table 1).

The contrasting patterns for $\delta^{13}C$ and $\delta^{15}N$ values in foliar materials can be made visible by considering the relationship between them (Fig. 3). The four sites are clearly separated in their $\delta^{15}N$ composition in foliar materials, even when showing all species together, which is not the case for $\delta^{13}C$. Slightly negative relationships were observed for suburban and urban sites for poplar, e.g., lower $\delta^{13}C$-values with increasing $\delta^{15}N$. The relationships between N concentrations in foliar materials and their $\delta^{15}N$-values were strong (Fig. 4, Table 1). When analysing the relationship between N% and $\delta^{15}N$ across all sites, significantly positive relationships were found for leaves of poplar ($p < 0.05$, $r^2 = 0.45$) and the needles of spruce ($p < 0.05$, $r^2 = 0.29$). The nitrogen content was also different between the species (Fig. 4, Table 1), with relatively low values for Scots pine (N = 1.4 ± 0.2%) and spruce (N = 1.4 ± 0.4%) compared to larch (N = 2.2 ± 0.4%), birch (N = 2.5 ± 0.3%) and poplar (N = 2.6 ± 0.4%).

The $\delta^{18}O$ values across all species and sites ranged between 17.3 and 29.9‰ with a mean value of 23.6 ± 2.4‰. Generally positive relationships were found between $\delta^{18}O$ and $\delta^{2}H$ values of foliar materials (Fig. 5), particularly strong for Scots pine ($r^2 = 0.57$, $p < 0.01$). These patterns were driven mostly by site differences, where both isotope compositions were generally enriched in the same order as Mt.A < Mt.B and suburban < urban, although this was not the case for poplar at urban and suburban sites. Hydrogen isotopic composition in the leaves of birch ($\delta^{2}H$ = -190 ± 8‰) showed the most depleted (negative) values at Mt.A compared to Mt.B ($\delta^{2}H$ = -166 ± 9‰). $\delta^{2}H$ was relatively enriched in the leaves of poplar at the suburban ($\delta^{2}H$ = -137 ± 13‰) and urban ($\delta^{2}H$ = -140 ± 18‰) sites. For the needles in larch there was a gradient along Mt.A, Mt.B, suburban and urban sites with $\delta^{2}H$ values of −182‰, −170‰, −163‰ and −157‰, respectively.

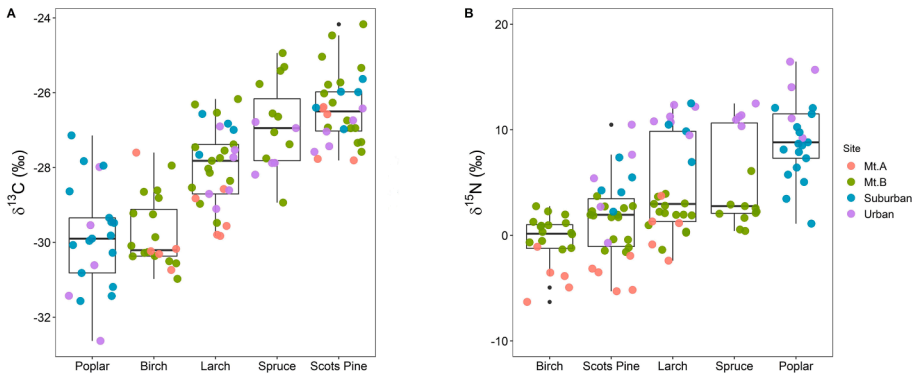

Fig. 2. Stable carbon isotope (A) and nitrogen isotope (B) composition in needle and leaf materials of the five tree species.

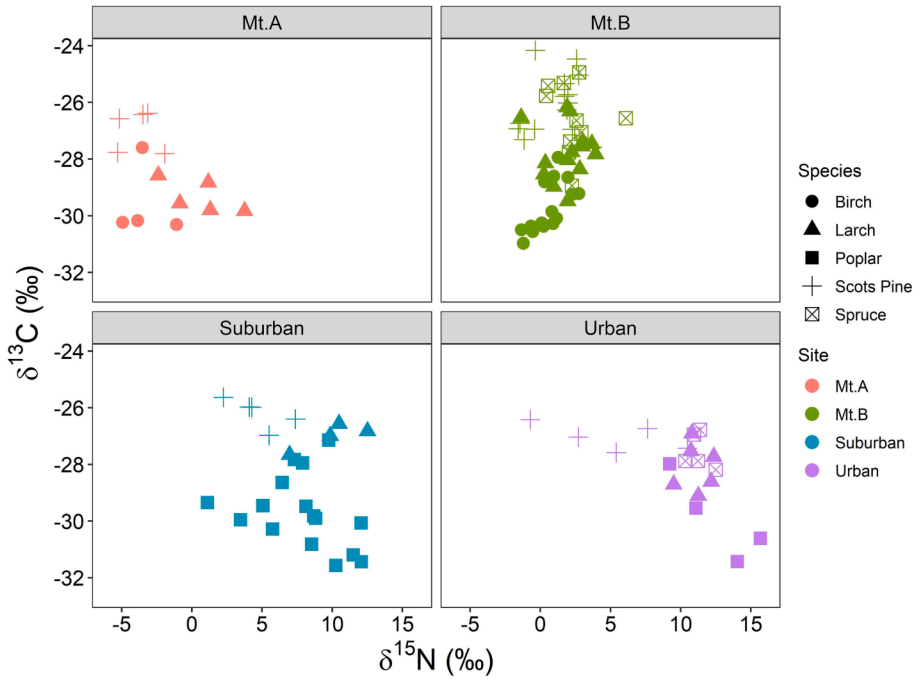

Fig. 3. Relationship between $\delta^{15}N$ and $\delta^{13}C$ values in leaves and needles for the different species and sites.

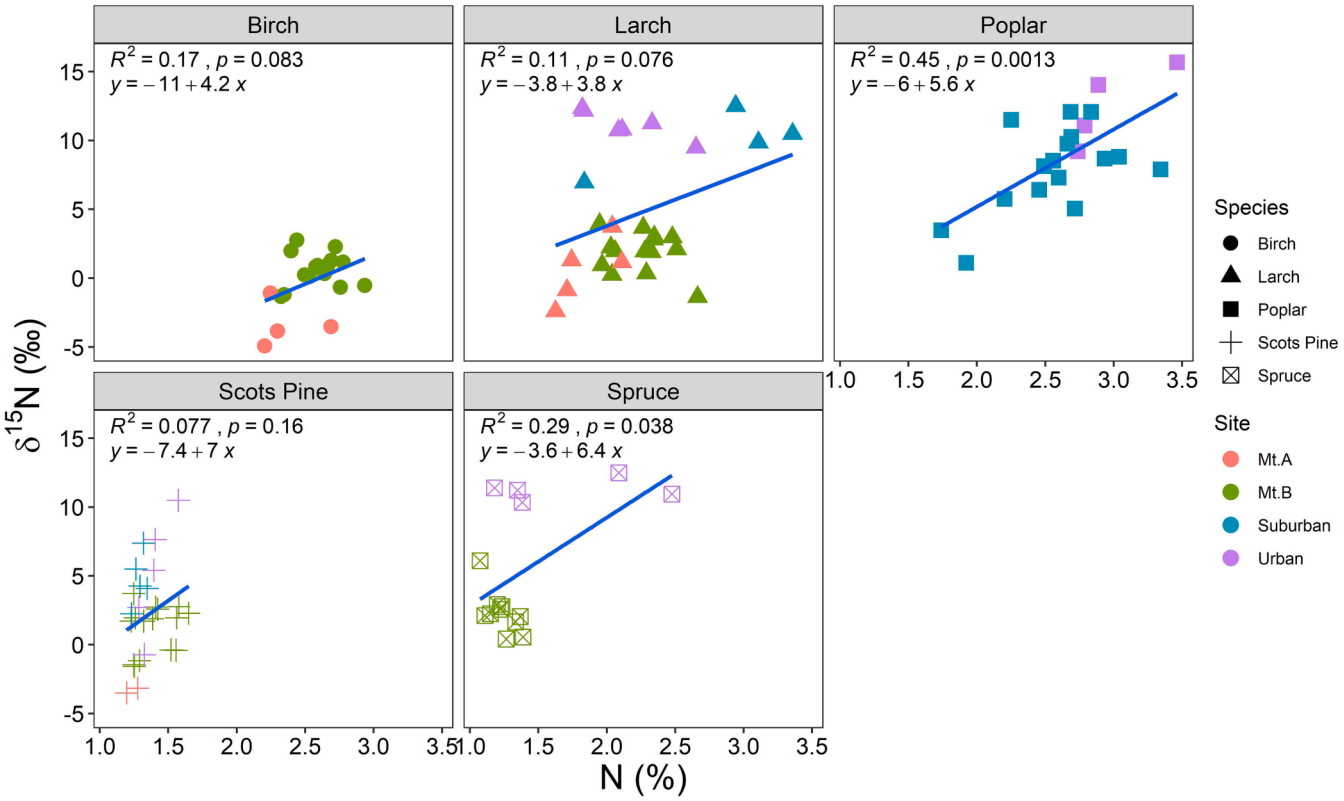

Fig. 4. Relationship between N concentration and $\delta^{15}N$ values in leaves and needles. Linear regression lines are indicted.

3.2. *Trace element composition of foliar materials*

Table 2 shows the concentrations of macro- and micro-elements in needles, highlighting the significant site differences for the investigated Scots pine and larch. The elements with the highest concentrations across all sites were Ca and K. The general order of the concentrations of both macro- (Al, Ca, Fe, Na and S) and micro-elements (B, Cr, Cu and Zn) in needles of larch was Mt.A < Mt.B < suburban < urban. For both species at Mt.A, the concentrations of Ni were below detection limit. The concentrations of Cd, Co, Mo and Pb were below detection limit in needles of two species at all four sites. Most prominent and significanty higher concentrations at the urban site were found for Al, B, Ca, Cr, Cu,

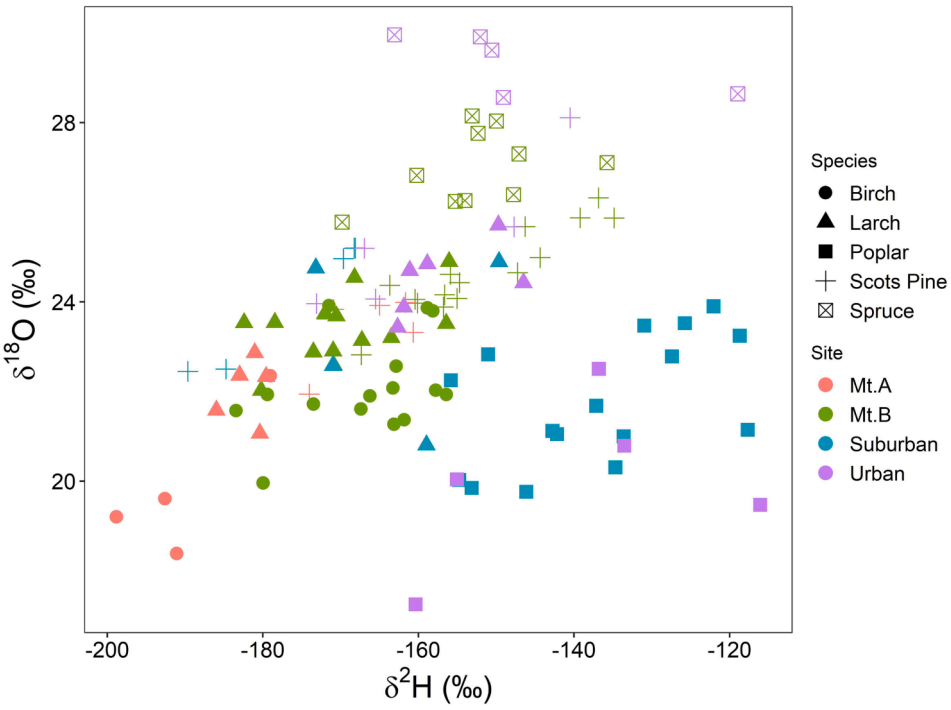

Fig. 5. Relationship between stable hydrogen and oxygen isotope compositions in leaves and needles.

Table 2
Chemical composition (mean ± standard deviation) of needles of Scots pine and larch from four sites. Significant differences between values of the least polluted site Mt.A and the other sites (Mt.B, Suburban, Urban) are shown in bold ($p < 0.05$).

	Scots pine				*Larch*			
	Mt.A	Mt.B	Suburban	Urban	Mt.A	Mt.B	Suburban	Urban
Macro-elements (mg/g)								
Al	0.6 ± 0.1	0.5 ± 0.2	0.9 ± 0.4	1.2 ± 1.0	0.5 ± 0.2	0.7 ± 0.3	**1.1 ± 0.3**	**2.2 ± 0.4**
Ca	3.7 ± 1.6	3.9 ± 1.1	5.5 ± 1.2	5.0 ± 2.8	5.2 ± 0.7	**6.5 ± 1.7**	10.4 ± 4.2	**8.5 ± 1.9**
Fe	0.3 ± 0.1	0.3 ± 0.1	**0.6 ± 0.3**	0.7 ± 0.5	0.3 ± 0.1	0.4 ± 0.2	**0.6 ± 0.2**	**1.6 ± 0.9**
K	4.8 ± 1.7	4.4 ± 0.9	3.8 ± 1.4	4.7 ± 1.8	6.4 ± 0.7	7.5 ± 1.7	6.1 ± 1.5	8.1 ± 1.9
Mg	1.1 ± 0.2	1.3 ± 0.3	1.4 ± 0.2	1.1 ± 0.2	2.2 ± 0.3	2.6 ± 0.7	2.9 ± 0.6	2.5 ± 0.5
Mn	0.3 ± 0.1	0.2 ± 0.1	**0.1 ± 0.1**	**0.1 ± 0.0**	0.3 ± 0.2	0.2 ± 0.1	**0.1 ± 0.0**	0.1 ± 0.0
Na	0.1 ± 0.0	0.1 ± 0.0	**1.2 ± 0.9**	**1.5 ± 0.9**	0.1 ± 0.0	0.1 ± 0.1	2.4 ± 1.5	**4.1 ± 2.4**
P	1.2 ± 0.1	1.2 ± 0.1	**0.9 ± 0.2**	1.1 ± 0.3	1.9 ± 0.2	2.1 ± 0.5	**1.4 ± 0.1**	1.8 ± 0.5
S	0.9 ± 0.1	**1.2 ± 0.2**	**1.2 ± 0.2**	**1.3 ± 0.2**	1.7 ± 0.1	**2.1 ± 0.2**	2.6 ± 0.7	**2.2 ± 0.3**
Micro-elements (µg/g)								
B	18.8 ± 7.7	**28.8 ± 6.9**	**41.1 ± 17.7**	24.6 ± 2.2	34.7 ± 11.7	**70.3 ± 12.5**	**108.2 ± 28.5**	**89.6 ± 27.0**
Ba	5.1 ± 1.9	4.9 ± 2.2	**14.2 ± 6.2**	19.4 ± 13.8	95.9 ± 17.4	81.6 ± 42.4	54.3 ± 39.4	94.0 ± 36.1
Cr	1.0 ± 0.1	1.1 ± 0.4	**1.4 ± 0.4**	1.9 ± 1.2	0.9 ± 0.2	1.0 ± 0.2	1.1 ± 0.4	**3.3 ± 1.7**
Cu	*DL*	3.9 ± 0.4	4.4 ± 0.5	5.7 ± 1.2	4.8 ± 0.6	4.9 ± 0.6	4.4 ± 0.5	**9.4 ± 2.7**
Zn	34.7 ± 11.5	30.9 ± 10.9	37.8 ± 10.5	42.3 ± 23.1	16.5 ± 2.4	**25.2 ± 7.1**	35.1 ± 21.5	**46.1 ± 15.5**

Fe, Na, S and Zn of both Scots pine and larch compared to the needles from the less polluted site Mt. A ($p < 0.05$). Across all sites, no significant difference for the concentrations of K and Mg in needles was found.

The Principal Component Analysis (PCA) including the variables concentration of Al, B, Ba, Ca, Cr, Cu, Fe, K, Mg, Mn, Na, P, S and Zn resulted in two principal components with eigenvalues > 1 and together account for 59.1% of the data variability for Scots pine and 53.8% for larch (Fig. 6). The two species were selected because data for all four sites were available. The biplot for Scots pine revealed that the two components differentiated the needles from remote site (Mt.A) to the two city sites (suburban and urban). Concentrations of Na, Fe, Ba, Al, Cr and Cu in needles from both suburban and urban sites had strong positive association with the first principal component.

For larch, the first principal component accounted for 37.7% of the total variance, combining the concentrations of Zn, Cu, Fe, Na, Cr and Al elements (Fig. 6b), while the second factor explained 16.1% of B, S, Mg and Ca variations. The needles of larch at suburban sites had significantly higher concentrations of Mg, Ca, S and B, while at the urban site higher concentrations of Cu, Cr, Fe, Zn, Na and Al ($p < 0.05$), but lower concentrations of Mn and P compared to both mountain sites were found.

3.3. Tree-ring carbon, nitrogen, and oxygen isotope chronologies

The temporal development from 1960 to 2019 for $\delta^{13}C$, $\delta^{15}N$ and $\delta^{18}O$ derived from the tree-ring data in 10-year resolution is shown for the studied conifer trees in Fig. 7. For $\delta^{13}C$, a general increase over time is observed for all species and sites, which is significant ($p < 0.05$) except for larch at the suburban site. This increase was somewhat more expressed at the beginning of the record compared to the later decades. The trends were very similar for all sites, with the exception of an offset to lower values observed for the site Mt.A. The overall range of values

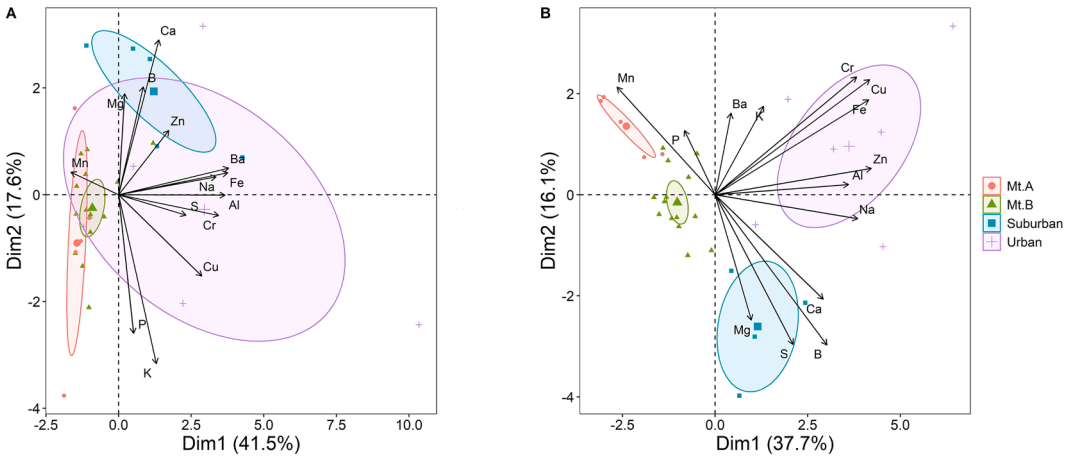

Fig. 6. Results of the principal component analysis using concentration of chemical elements in the needles of P. sylvestris (A) and L. sibirica (B).

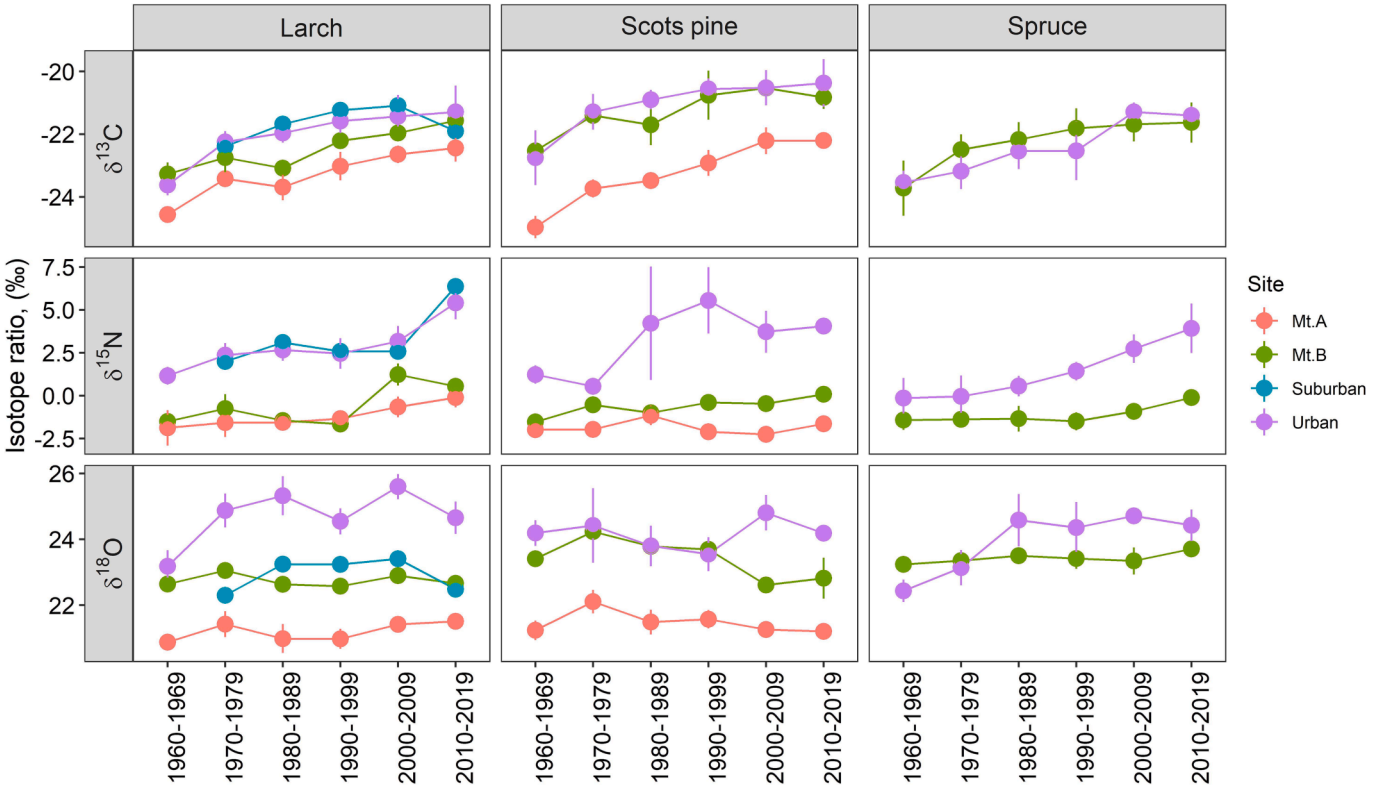

Fig. 7. Tree ring stable carbon, nitrogen and oxygen isotopes chronologies of the investigated conifers species.

was between −20.4‰ and −25.0‰ and therefore higher compared to the corresponding values of the needles by several ‰ (Table 1).

For $\delta^{15}N$ in the tree rings, there was a clear separation between values for Mt.A and B in comparison to suburban and urban sites, both in terms of absolute values as well as temporal trends. The chronologies from Mt.A and B did not show changes over time, whereas this was clearly the case for urban spruce and Scots pine trees, as well as urban and suburban larch trees. Comparing averages of the first two and last two decades across all species, we observed a highly significant increase ($p < 0.01$) from 1.0‰ ± 0.9‰ to 4.9‰ ± 1.1‰ for the urban and suburban sites. In contrast, the range of $\delta^{15}N$ values at Mt.A and B was around zero or in the negative range for all species and time points.

The $\delta^{18}O$ chronologies showed the most distinct differences between the sites of all isotope ratios, but no significant temporal trends. For instance for larch for the most recent period, mean $\delta^{18}O$ values (mean ± SD) were found 21.3 ± 0.3‰, 22.7 ± 0.2‰ and 23.0 ± 0.5‰ at Mt.A, Mt.B and suburban, respectively, while 24.9 ± 0.6‰ for the urban site. Similarly for Scots pine, the mean $\delta^{18}O$ values over the period 1990–2019, it was 21.4 ± 0.2‰ and 23.0 ± 0.6‰ at Mt.A and Mt.B, respectively, but more enriched at urban sites (24.2 ± 0.6‰). Also for spruce, mean urban $\delta^{18}O$ values of 23.5 ± 0.2‰ were higher than at Mt. B (24.5 ± 0.2‰) (only these two sites available).

4. Discussion

Clear differences in nitrogen isotope ratios and trace elemental compositions in needles and tree rings at urban and suburban sites compared to the more remote mountainous locations could indicate an air pollution effect. The stable isotope ratios of carbon, oxygen and hydrogen were found to reflect a physiological response of the

vegetation to the pollution, super-imposed by the impact of climatic factors. Our multi-isotope and multi-element approach therefore enables to infer information on pollution as well as their effects on the forest ecosystems. In the following, we discuss these findings in two parts.

4.1. Influence of pollution

Our $\delta^{15}N$ results clearly show isotopically enriched values in needles and leaves of trees near pollution sources. The most negative and lowest values of $\delta^{15}N$ were recorded in birch, larch and Scots pine at the remote site Mt.A, while the highest $\delta^{15}N$ values were measured at the two city sites. In suburban and urban sites, $\delta^{15}N$ reached unusually high values of more than + 10‰ in larch, poplar and spruce (urban only), and about half of this enrichment in Scots pine (Table 1). The main source of air pollution is likely generated by "Ger district", which is settled between Mt.A and the city center (Davy et al. 2011). Considering the frequent wind direction from the north and northwest, the released air pollutants from Ger district and the city are expected to be transferred by wind to the north slope of Mt.B which therefore could receive more pollution than Mt.A (Fig. 1). This was indeed the case (Table 1).

Although we did not measure $\delta^{15}N$ of atmospheric compounds (NO_x), several studies have reported anthropogenic sources to often emit relatively ^{15}N-enriched compounds that can be caused by fractionation in combustion processes (Savard et al. 2023). $\delta^{15}N$ of NO_2 can be as high as + 10.2 to + 16.9‰ and is taken up by tree leaves and needles (Cobley and Pataki 2019; Saurer et al. 2004), consistent with our results. It needs to be considered that only a small fraction of nitrogen used by the plants originates directly from atmospheric uptake through stomatal openings, but the main source is nitrogen from the soil (Högberg et al. 2006). Processes affecting isotope ratios in the soil have a multitude of causes and reflect nitrogen cycling dynamics (Mathias and Thomas 2018). However, it was also shown that long-term exposition to pollution can lead to a similar enrichment in soil as in the canopy (Savard et al. 2023). Leaves and needles are falling to the ground and after microbial decomposition, this nitrogen is re-used by the plants albeit after isotope fractionation (McLauchlan and Craine 2012). An uncertainty in our interpretation is certainly involved in the comparison of different sites with different soil conditions. Therefore, ^{15}N isotope differences between sites could have other causes than the differential exposition to nitrogen pollution. However, we have several pieces of evidence for deriving a pollution signal from results, namely the relationship with nitrogen content as well as the temporal development derived from the tree rings.

The pollution signal derived from the needle results is further confirmed by patterns observed in the total nitrogen content. In needles of larch, N concentrations show a clear pattern across all four sites, with higher values in suburban and urban than in the two mountain sites. The relationships between $\delta^{15}N$ values and N concentrations were positively related in leaves of poplar and the needles of spruce, whereas no correlation was observed with needles of Scots pine (Fig. 4), thus possibly indicating less impact and uptake of nitrogen pollution for this species.

The pattern of enriched $\delta^{15}N$ values at urban and suburban sites compared to the more remote sites was also observed in the tree-ring analysis (Fig. 7). Values from Mt.A and B were generally below zero and not changing over the recent decades. In contrast, for the urban sites, where data are available for all three species, not only higher $\delta^{15}N$ values were observed, but also an increasing trend over time, reflected in a significant increase when comparing the early period (1960–1979) to the more recent one (2000–2019). There were differences in temporal pattern for the three tree species, which may be related to different biological factors impacting the incorporated N (Saurer et al. 2004). Trends in nitrogen isotope ratios over time based on tree rings are often not easy to interpret because of the many isotope fractionations involved, particularly in the soil (McLauchlan and Craine 2012; Savard et al. 2023). Overall, our tree-ring results are at least consistent with increasing nitrogen pollution load deposited on the forests, although other causes cannot be excluded.

The PCA biplot results indicated that microelements emitted from the traffic activities like B, Co, Cr, Cu, Fe, Ni and Zn dominated in the two city sites (Fig. 6), possibly with contributions also from industrial emissions and soil dust (Kardel et al. 2018). Toxic elements such as Al and Zn, which are known to be negatively associated with tree growth (Locosselli et al. 2019), were found at elevated concentrations in the urban environments. The microelement analysis and evaluation in our study therefore clearly showed the impact of air pollution on trees growing in urban and suburban sites. In particular, chemical elements typical for vehicular emissions and tire abrasion showed higher concentrations in areas with higher traffic intensity and busy streets in the city. As a consequence, city trees may accumulate particulate matter (PM) including $PM_{2.5}$ and PM_{10} on the leaf surface (Moreira et al., 2016). This accumulation can change the leaves' optical properties, increase leaf temperature and reduce light availability for photosynthesis (Siegwolf et al. 2022). Furthermore, high accumulation rates of PM may reduce the potential gas exchanges due to partial blockage of leaf stomata. In Ulaanbaatar city, the coldest and most polluted months span from end of December to January with low precipitation. During that time, the concentration of PM reaches the highest values. The deposition of PM on the leaves and subsequent incorporation during low precipitation periods may adversely affect the concentration of non-structural carbohydrates (NSC) also later during the growing season, leading to a reduced photosynthetic capacity. The harsh climate conditions as a main driver of growth variability in this region together with the strong effect of air pollution may negatively impact the health of urban trees (Locosselli et al. 2019). These joint effects of climate change and increasing pollution are therefore expected to have discernible physiological effects, as discussed in detail in the following section.

4.2. Physiological responses

The $\delta^{13}C$ values in plant compounds reflect the signature of (1) the source of plant carbon, i.e., atmospheric CO_2, and (2) the isotope fractionation effects during photosynthesis (Farquhar et al. 1989). Therefore, variations between sites, species and over time can be interpreted with regard to these two principal factors. The carbon isotope composition of CO_2 produced by gasoline combustion is depleted relative to background atmospheric CO_2, such that urban atmospheric CO_2 can be more depleted in ^{13}C than CO_2 of rural locations (Freyer 1979). Therefore, any significant uptake of this pollution-derived depleted CO_2 could also result in relatively depleted values of either needles and/or tree rings. However, for the $\delta^{13}C$ values of foliar materials in our study, we found no clear patterns across all four sites, but rather species-specific differences were dominant (Fig. 2a). In the tree rings, even the opposite was observed, as values from urban and suburban sites were enriched compared to values from Mt.A (Fig. 7). This indicates that an isotopic fingerprint of increased CO_2 concentrations from fossil fuel emissions could not be detected, but that rather physiological effects were dominant in shaping the $\delta^{13}C$ patterns. When photosynthetic capacity or stomatal conductance are hampered, this affects the ^{13}C isotope discrimination and subsequently the carbon isotope ratio of organic materials (Farquhar et al. 1989). Such effects are possible because of both pollution and climate. For instance, stable carbon isotope ratios were shown to be affected by strong SO_2 pollution (Savard et al. 2004), likely through effects on photosynthesis, with stressed plants often showing increased values (Siegwolf et al. 2022). Furthermore, the influence of environmental factors such as temperature, water supply, and CO_2 concentration are generally reflected in plant $\delta^{13}C$ values. Organic $\delta^{13}C$ values become lower with increasing water availability, including average rainfall, while the opposite occurs under plant drought stress. The enriched tree-ring $\delta^{13}C$ values at urban and suburban sites may therefore indicate increased plant stress, but it is not possible from our data alone to infer the cause as pollution or climate. Furthermore, the increasing $\delta^{13}C$ trend over time indicates increasing plant

stress, that would be consistent with an increasing pollution load.

According to the Information and Research Institute of Meteorology, Hydrology and Environment (IRIMHE) of Mongolia, the climate also has changed significantly since 1940: mean annual temperature (MAT) increased by 1.04 °C. There is in fact a correlation between the temperature trend and the tree-ring $\delta^{13}C$-trends of all species and sites, which are, however, not statistically significant because of our grouping of data into 10-yr blocks. Mean annual precipitation (MAP) decreased by 10% between 1960 and 2019, particularly from the 1990 s on in Ulaanbaatar. These changes in MAT and MAP increased the intensity and frequency of droughts, especially during the growing season, as expressed with the drought index SPEI. Severe droughts occurred in 2007 (SPEI −1.43) and 2015 (SPEI −1.44). An influence of drought on carbon isotope ratios in tree rings has often been observed (Savard and Daux 2020). A recent tree-ring study in Central Mongolia also confirmed these climate and related isotope changes (Leland et al. 2023). We must therefore assume a combined effect of climate and pollution on urban and suburban trees. This can also result in a disturbance of the normal climate-tree growth relationship as has been reported in Europe for silver fir (Boettger et al., 2014).

The stable isotope compositions of δ^2H and $\delta^{18}O$ can potentially help to identify better the causes of tree physiological changes as were described above. δ^2H and $\delta^{18}O$ values were found to be lower in the leaves and needles of all species at the most distant site Mt.A compared to Mt.B and the two city sites. The oxygen isotope composition in plant materials has been well studied and shown to be affected mainly by the isotope composition of soil water (and thus precipitation) and transpiration processes at the leaf level. The leaf water enrichment is mainly driven by changes in relative humidity, air temperature, and by the isotopic composition of the water vapour but also by plant physiological parameters such as leaf temperature, stomatal conductance, and transpiration rate (Allen et al. 2013; Cernusak et al. 2016). Because atmospheric CO_2 entering the stomatal cavity rapidly equilibrates with leaf water, it is expected that the isotopic signal of leaf water is imprinted on $\delta^{18}O$ of organic compounds during photosynthetic CO_2 assimilation (Lehmann et al., 2017). The observed low values at the remote site Mt.A, however, may be mainly caused by climatic and altitudinal differences to the city, that influenced the isotope signal of precipitation and thus water the trees take up. Oxygen isotope variations in tree-rings have often been successfully related to temperature and drought (Büntgen et al. 2021; Savard and Daux 2020), but in our study we could not establish a clear link, maybe related to the relatively low temporal resolution in our data. Similarly to $\delta^{18}O$, the environmental effects on transpiration and evaporation can drive the δ^2H enrichment in leaf water and in the plant organs. High correlation between $\delta^{18}O$ and δ^2H in organic matter indicates that the water of source and environmental effects dominate the isotope fractionation, whereas a lack of correlation suggests an additional hydrogen or oxygen isotope fractionation effect during biochemistry (Lehmann et al. 2021; Vitali et al. 2022). Therefore, it must be assumed that leaf δ^2H is not only affected by changes in transpiration and stomatal conductance, alongside the evaporative conditions, but also by photosynthetic reactions and carbon metabolism in plants (Cormier et al. 2018; Holloway-Phillips et al., 2022). The observed correlation between $\delta^{18}O$ and δ^2H in leaves and needles for our study sites suggests a dominant role of climatic over biochemical controls.

5. Conclusion

In this study, five main tree species in the Ulaanbaatar region were used to evaluate the effect of air pollution on the growth of urban vs. non-urban mountain trees. With our multi-isotope and multi-element approach, we found likely effects of air pollution with higher $\delta^{15}N$ and accumulated higher concentrations of various trace elements in trees of the (sub-)urban compared to the mountain sites. We also investigated how this pollution affected the trees on a physiological level and the interaction of pollution with climate changes by analysis of $\delta^{13}C$, $\delta^{18}O$ and δ^2H. While needle values reflect the current situation, the tree-ring data complement the information by putting this status in a long-term context. Our data and comparison of different sites suggested climatic changes to be dominant over pollution effects for forest health in the region. A great demand for such information exists, especially in view of new hot spots of pollution arising not only in Mongolia, but also in other Asian countries, due to ongoing industrialization processes and demographic developments. The gained knowledge will serve decision makers to better adapt future forest management practices.

CRediT authorship contribution statement

Enkh-Uchral Batkhuyag: Conceptualization, Methodology, Formal analysis, Writing – original draft. **Marco M. Lehmann:** Methodology, Writing – review & editing. **Paolo Cherubini:** Conceptualization, Writing – review & editing. **Bilguun Ulziibat:** Methodology, Formal analysis. **Tseren-Ochir Soyol-Erdene:** Conceptualization, Methodology, Supervision, Writing – review & editing. **Marcus Schaub:** Conceptualization, Supervision, Writing – review & editing. **Matthias Saurer:** Methodology, Writing – review & editing.

Declaration of Competing Interest

The authors declare that they have no known competing financial interests or personal relationships that could have appeared to influence the work reported in this paper.

Data availability

Data will be made available on request.

Acknowledgements

The research has been initiated through collaboration of ICP Forests and EANET and was conducted during a fellowship supported by the Swiss Government Excellence Scholarships for E-UB. The graduate students' scholarship from Ministry of Environment and Tourism of Mongolia was supported for Bilguun (MNG-RS-004). MML was supported by the SNF Ambizione grant (No. 179978). We also thank Manuela Oettli for the technical support in the Stable Isotope Research Centre at WSL.

References

Allen, R.W., Gombojav, E., Barkhasragchaa, B., Byambaa, T., Lkhasuren, O., Amram, O., Takaro, T.K., Janes, C.R., 2013. An assessment of air pollution and its attributable mortality in Ulaanbaatar, Mongolia. Air Qual. Atmos. Health 6 (1), 137–150.

Austruy, A., Yung, L., Ambrosi, J.P., Girardclos, O., Keller, C., Angeletti, B., Dron, J., Chamaret, P., Chalot, M., 2019. Evaluation of historical atmospheric pollution in an industrial area by dendrochemical approaches. Chemosphere 220, 116–126.

Ballikaya, P., Marshall, J., Cherubini, P., 2022. Can tree-ring chemistry be used to monitor atmospheric nanoparticle contamination over time? Atmos. Environ. 268, 118781.

Ballikaya, P., Brunner, I., Cocozza, C., Grolimund, D., Kaegi, R., Murazzi, M.E., Schaub, M., Schoenbeck, L.C., Sinnet, B., Cherubini, P., 2023. First evidence of nanoparticle uptake through leaves and roots in beech (*Fagus sylvatica* L.) and pine (*Pinus sylvestris* L.). Tree Physiology. 43, 262–276.

Barabad, M., Jung, W., Versoza, M., Kim, M., Ko, S., Park, D., Lee, K., 2018. Emission characteristics of particulate matter, volatile organic compounds, and trace elements from the combustion of coals in Mongolia. Int. J. Environ. Res. Public Health 15, 1706.

Belmecheri, S., Lavergne, A., 2020. Compiled records of atmospheric CO_2 concentrations and stable carbon isotopes to reconstruct climate and derive plant ecophysiological indices from tree rings. Dendrochronologia 63, 125748.

Boettger, T., Haupt, M., Friedrich, M., 2014. Reduced climate sensitivity of carbon, oxygen and hydrogen stable isotope ratios in tree-ring cellulose of silver fir (*Abies alba* Mill.) influenced by background SO_2 in Franconia (Germany, Central Europe). Environmental Pollution 185, 281–294.

Büntgen, U., Urban, O., Krusic, P.J., Rybníček, M., Kolář, T., Kyncl, T., Ač, A., Koňasová, E., Čáslavský, J., Esper, J., Wagner, S., Saurer, M., Tegel, W.,

Dobrovolný, P., Cherubini, P., Reinig, F., Trnka, M., 2021. Recent European drought extremes beyond common era background variability. Nat. Geosci. 14 (4), 190–196.
Cailleret, M., Ferretti, M., Gessler, A., Rigling, A., Schaub, M., Cao, K.-F., 2018. Ozone effects on European forest growth-towards an integrative approach. J. Ecol. 106 (4), 1377–1389.
Cernusak, L.A., Barbour, M.M., Arndt, S.K., Cheesman, A.W., English, N.B., Feild, T.S., Helliker, B.R., Holloway-Phillips, M.M., Holtum, J.A.M., Kahmen, A., McInerney, F. A., Munksgaard, N.C., Simonin, K.A., Song, X., Stuart-Williams, H., West, J.B., Farquhar, G.D., 2016. Stable isotopes in leaf water of terrestrial plants: stable isotopes in leaf water. Plant Cell Environ. 39 (5), 1087–1102.
Cherubini, P., Battipaglia, G., Innes, J.L., 2021. Tree vitality and forest health: can tree-ring stable isotopes be used as indicators? Current Forestry Reports. 7, 69–80.
Cobley, L.A.E., Pataki, D.E., 2019. Vehicle emissions and fertilizer impact the leaf chemistry of urban trees in Salt Lake Valley. UT. Environmental Pollution. 254, 112984.
Cocozza, C., Perone, A., Giordano, C., Salvatici, M.C., Pignattelli, S., Raio, A., Schaub, M., Sever, K., Innes, J.L., Tognetti, R., Cherubini, P., Steppe, K., 2019. Silver nanoparticles enter the tree stem faster through leaves than through roots. Tree Physiol. 39 (7), 1251–1261.
Cormier, M.-A., Werner, R.A., Sauer, P.E., Gröcke, D.R., Leuenberger, M.C., Wieloch, T., Schleucher, J., Kahmen, A., 2018. ^{2}H-fractionations during the biosynthesis of carbohydrates and lipids imprint a metabolic signal on the δ^{2}H values of plant organic compounds. New Phytol. 218 (2), 479–491.
Cutter, B.E., Guyette, R.P., 1993. Anatomical, chemical and ecological factors affecting tree species choice in dendrochemistry studies. J. Environ. Qual. 22 (3), 611–619.
Davy, P.K., Gunchin, G., Markwitz, A., Trompetter, W.J., Barry, B.J., Shagjjamba, D., Lodoysamba, S., 2011. Air particulate matter pollution in Ulaanbaatar, Mongolia: determination of composition, source contributions and source locations. Atmos. Pollut. Res. 2 (2), 126–137.
Dinis, L., Bégin, C., Savard, M.M., Parent, M., 2021. Impacts of smelter atmospheric emissions on forest nutrient cycles: evidence from soils and tree rings. Sci. Total Environ. 751, 141427.
Dulamsuren, C., Hauck, M., Leuschner, C., 2009. Recent drought stress leads to growth reductions in Larix sibirica in the western Khentey Mongolia. Global Change Biol. 16, 3024–3035.
Farquhar, G.D., Ehleringer, J.R., Hubick, K.T., 1989. Carbon isotope discrimination and photosynthesis. Annu. Rev. Plant. Physiol. Plant. Mol. Biol. 40 (1), 503–537.
Freyer, H.D., 1979. C-13 record in tree rings. 2. registration of micro-environmental CO_2 and anomalous pollution effect. Tellus 31, 308–312.
Ganbat, G., Soyol-Erdene, T.-O., Jadamba, B., 2020. Recent improvement in particulate matter (PM) pollution in Ulaanbaatar, Mongolia. Aerosol and Air Quality Research. 20 (10), 2280–2288.
Gerschlauer, F., Saiz, G., Schellenberger Costa, D., Kleyer, M., Dannenmann, M., Kiese, R., 2019. Stable carbon and nitrogen isotopic composition of leaves, litter, and soils of various ecosystems along an elevational and land-use gradient at Mount Kilimanjaro, Tanzania. Biogeosciences. 16, 409–424.
Griffiths, H., 2020. Stable Isotopes: Integration of biological, ecological and geochemical processes, 1 Edn. Garland Science.
Guyette, R.P., Cutter, B.E., Henderson, G.S., 1991. Long-term correlations between mining activity and levels of lead and cadmium in tree-rings of Eastern red-cedar. J. Environ. Qual. 20 (1), 146–150.
Hauck, M., Dulamsuren, C., Leuschner, C., 2016. Anomalous increase in winter temperature and decline in forest growth associated with severe winter smog in the Ulan Bator Basin. Water Air Soil Pollut. 227, 261.
Hessl, A.E., Anchukaitis, K.J., Jelsema, C., Cook, B., Byambasuren, O., Leland, C., Nachin, B., Pederson, N., Tian, H., Hayles, L.A., 2018. Past and future drought in Mongolia. Sci. Adv. 4, e1701832.
Högberg, P., Fan, H.B., Quist, M., Binkley, D., Tamm, C.O., 2006. Tree growth and soil acidification in response to 30 years of experimental nitrogen loading on boreal forest. Glob. Chang. Biol. 12, 489–499.
Högberg, P., Johannisson, C., Yarwood, S., Callesen, I., Näsholm, T., Myrold, D.D., Högberg, M.N., 2011. Recovery of ectomycorrhiza after 'nitrogen saturation' of a conifer forest. New Phytol. 189 (2), 515–525.
Holloway-Phillips, M., Baan, J., Nelson, D.B., Lehmann, M.M., Tcherkez, G., Kahmen, A., 2022. Species variation in the hydrogen isotope composition of leaf cellulose is mostly driven by isotopic variation in leaf sucrose. Plant Cell Environ. 45 (9), 2636–2651.
Holmes, R.L., 1983. Program COFECHA User's Manual. The University of Arizona, Tucson, Laboratory of Tree-Ring Research.
Juřička, D., Kusbach, A., Pařílková, J., Houška, J., Ambrožová, P., Pecina, V., Rosická, Z., Brtnický, M., Kynický, J., 2020. Evaluation of natural forest regeneration as a part of land restoration in the Khentii massif, Mongolia. J. Forestry Res. 31 (5), 1773–1786.
Kardel, F., Wuyts, K., De Wael, K., Samson, R., 2018. Biomonitoring of atmospheric particulate pollution via chemical composition and magnetic properties of roadside tree leaves. Environ. Sci. Pollut. Res. 25 (26), 25994–26004.
Kolář, T., Kusbach, A., Čermák, P., Štěrba, T., Batkhuu, E., Rybníček, M., 2020. Climate and wildfire effects on radial growth of *Pinus sylvestris* in the Khan Khentii Mountains, north-central Mongolia. J. Arid Environ. 182, 104223.
Kress, A., Saurer, M., Siegwolf, R.T.W., Frank, D.C., Esper, J., Bugmann, H., 2010. A 350 year drought reconstruction from Alpine tree ring stable isotopes. Global Biogeochem. Cycles 24 (2), n/a–n/a.
Lehmann, M.M., Gamarra, B., Kahmen, A., Siegwolf, R.T.W., 2017. Oxygen isotope fractionations across individual leaf carbohydrates in grass and tree species. Plant, Cell & Environment 40, 1658–1670.
Lehmann, M.M., Vitali, V., Schuler, P., Leuenberger, M., Saurer, M., 2021. More than climate: Hydrogen isotope ratios in tree rings as novel plant physiological indicator for stress conditions. Dendrochronologia 65, 125788.
Leland, C., Andreu-Hayles, L., Cook, E.R., Anchukaitis, K., Byambasuren, O., Davi, N., Hessl, A., Martin-Benito, D., Nachin, B., Pederson, N., 2023. Impacts of climate and tree morphology on tree-ring stable isotopes in Central Mongolia. Tree Physiology. 43, 539–555.
Lelieveld, J., Evans, J.S., Fnais, M., Giannadaki, D., Pozzer, A., 2015. The contribution of outdoor air pollution sources to premature mortality on a global scale. Nature 525 (7569), 367–371.
Locosselli, G.M., Camargo, E.P.d., Moreira, T.C.L., Todesco, E., Andrade, M.d.F., André, C.D.S.d., André, P.A.d., Singer, J.M., Ferreira, L.S., Saldiva, P.H.N., Buckeridge, M.S., 2019. The role of air pollution and climate on the growth of urban trees. Sci. Total Environ. 666, 652–661.
Maher, B.A., Moore, C., Matzka, J., 2008. Spatial variation in vehicle-derived metal pollution identified by magnetic and elemental analysis of roadside tree leaves. Atmos. Environ. 42 (2), 364–373.
Mathias, J.M., Thomas, R.B., 2018. Disentangling the effects of acidic air pollution, atmospheric CO_2, and climate change on recent growth of red spruce trees in the Central Appalachian Mountains. Glob. Chang. Biol. 24, 3938–3953.
McLauchlan, K.K., Craine, J.M., 2012. Species-specific trajectories of nitrogen isotopes in Indiana hardwood forests, USA. Biogeosciences. 9, 867–874.
McLaughlin, S.B., Shortle, W.C., Smith, K.T., 2002. Dendroecological applications in air pollution and environmental chemistry: research needs. Dendrochronologia 20 (1-2), 133–157.
Moreira, T.C.L., de Oliveira, R.C., Amato, L.F.L., Kang, C.-M., Saldiva, P.H.N., 2016. Intra-urban biomonitoring: Source apportionment using tree barks to identify air pollution sources. Environment International 91, 271–275.
Newman, S., Xu, X., Affek, H.P., Stolper, E., Epstein, S., 2008. Changes in mixing ratio and isotopic composition of CO 2 in urban air from the Los Angeles basin, California, between 1972 and 2003. J. Geophys. Res. 113 (D23).
Nishikawa, M., Matsui, I., Batdorj, D., Jugder, D., Mori, I., Shimizu, A., Sugimoto, N., Takahashi, K., 2011. Chemical composition of urban airborne particulate matter in Ulaanbaatar. Atmos. Environ. 45 (32), 5710–5715.
Rautio, P., A. Fürst, K. Stefan, H. Raitio and U. Bartels. 2020. Part XII: Sampling and analysis of needles and leaves. in manual on methods and criteria for harmonized sampling, assessment, monitoring and analysis of the effects of air pollution on forests, Thünen Institute of Forest Ecosystems, Eberswalde, Germany, p 19.
R-Core-Team R: A language and environment for statistical computing 2020.
Salehi, M., Walthert, L., Zimmermann, S., Waldner, P., Schmitt, M., Schleppi, P., Liechti, K., Ahmadi, M., Zahedi Amiri, G., Brunner, I., Thimonier, A., 2020. Leaf morphological traits and leaf nutrient concentrations of European beech across a water availability gradient in Switzerland. Front. Forests Global Change. 3, 19.
Sase, H., Bulgan, T., Batchuluun, T., Shimizu, H., Totsuka, T., 2005. Tree Decline and its Possible Causes around Mt Bogdkhan in Mongolia. Phyton-Annales Rei Botanicae. 45, 583–590.
Saurer, M., Cherubini, P., Ammann, M., De Cinti, B., Siegwolf, R., 2004. First detection of nitrogen from NOx in tree rings: a $^{15}N/^{14}N$ study near a motorway. Atmos. Environ. 38 (18), 2779–2787.
Savard, M.M., Bégin, C., Parent, M., Smirnoff, A., Marion, J., 2004. Effects of smelter sulfur dioxide emissions: a spatiotemporal perspective using carbon isotopes in tree rings. J. Environ. Qual. 33 (1), 13–26.
Savard, M.M., Daux, V., 2020. An overview on isotopic divergences - causes for instability of tree-ring isotopes and climate correlations. Clim. Past 16, 1223–1243.
Savard, M.M., Marion, J., Bégin, C., Laganière, J., 2023. On the significance of long-term trends in tree-ring N isotopes-the interplay of soil conditions and regional NOx emissions. Sci. Total Environ. 857, 159580.
Schuler, P., Cormier, M.-A., Werner, R.A., Buchmann, N., Gessler, A., Vitali, V., Saurer, M., Lehmann, M.M., 2022. A high-temperature water vapor equilibration method to determine non-exchangeable hydrogen isotope ratios of sugar, starch and cellulose. Plant Cell Environ. 45 (1), 12–22.
Siegwolf, R.T.W., Matyssek, R., Saurer, M., Maurer, S., Günthardt-Goerg, M.S., Schmutz, P., Bucher, J.B., 2001. Stable isotope analysis reveals differential effects of soil nitrogen and nitrogen dioxide on the water use efficiency in hybrid poplar leaves. New Phytol. 149 (2), 233–246.
Takahashi, M., Feng, Z., Mikhailova, T.A., Kalugina, O.V., Shergina, O.V., Afanasieva, L. V., Heng, R.K.J., Majid, N.M.A., Sase, H., 2020. Air pollution monitoring and tree and forest decline in East Asia: a review. Sci. Total Environ. 742, 140288.
UNICEF. 2018. Mongolia's air pollution crisis: A call to action to protect children's health.
Visser, S., Slowik, J.G., Furger, M., Zotter, P., Bukowiecki, N., Canonaco, F., Flechsig, U., Appel, K., Green, D.C., Tremper, A.H., Young, D.E., Williams, P.I., Allan, J.D., Coe, H., Williams, L.R., Mohr, C., Xu, L., Ng, N.L., Nemitz, E., Barlow, J.F., Halios, C. H., Fleming, Z.L., Baltensperger, U., Prevot, A.S.H., 2015. Advanced source apportionment of size-resolved trace elements at multiple sites in London during winter. Atmos. Chem. Phys. 15, 11291–11309.
Vitali, V., Martínez-Sancho, E., Treydte, K., Andreu-Hayles, L., Dorado-Liñán, I., Gutierrez, E., Helle, G., Leuenberger, M., Loader, N.J., Rinne-Garmston, K.T., Schleser, G.H., Allen, S., Waterhouse, J.S., Saurer, M., Lehmann, M.M., 2022. The

unknown third – hydrogen isotopes in tree-ring cellulose across Europe. Sci. Total Environ. 813, 152281.
Siegwolf, R.T.W., M.M. Savard, T.E.E. Grams and S. Voelker. 2022. Impact of Increasing CO2, and Air Pollutants (NOx, SO2, O3) on the Stable Isotope Ratios in Tree Rings. In Stable Isotopes in Tree Rings: Inferring Physiological, Climatic and Environmental Responses Eds. R.T.W. Siegwolf, J.R. Brooks, J. Roden and M. Saurer. Springer International Publishing, Cham, pp 675-710.
WHO, 2019. Air pollution in Mongolia. Bull. World Health Organ. 97, 79–80.